SUPPLEMENTARY DATA

GDNF-RET signaling in ER-positive breast cancers is a key determinant of response and resistance to aromatase inhibitors

Andrea Morandi, Lesley-Ann Martin, Qiong Gao, Sunil Pancholi, Alan Mackay, David Robertson, Marketa Zvelebil, Mitch Dowsett, Ivan Plaza-Menacho and Clare M. Isacke

The SUPPLEMENTARY DATA contains:

Supplementary Figures 1-8

Supplementary Table 1
is provided as an excel files (.xlsx) and containing multiple tabs:

A. GSEA analysis

B. GDNF-RGS gene list

C. GO analysis

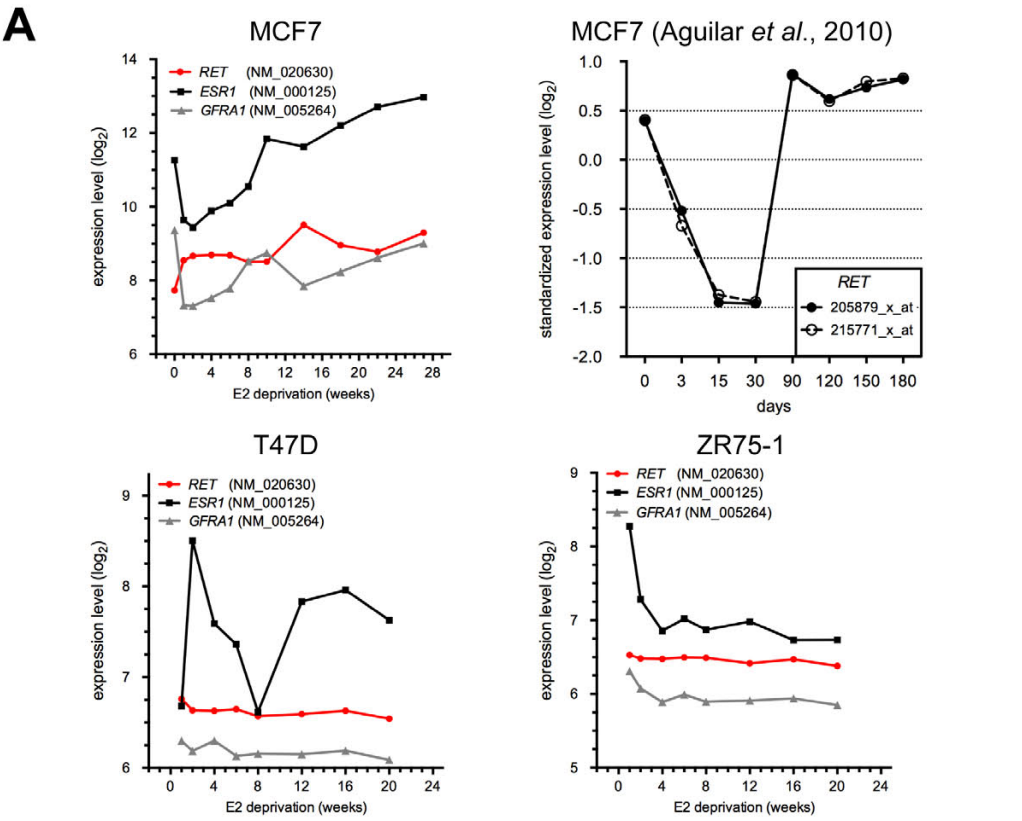
A
MCF7
RET (NM_020630)
ESR1 (NM_000125)
GFRA1 (NM_005264)
expression level (log2)
E2 deprivation (weeks)
MCF7 (Aguilar et al., 2010)
standardized expression level (log2)
RET
205879_x_at
215771_x_at
days
T47D
ZR75-1

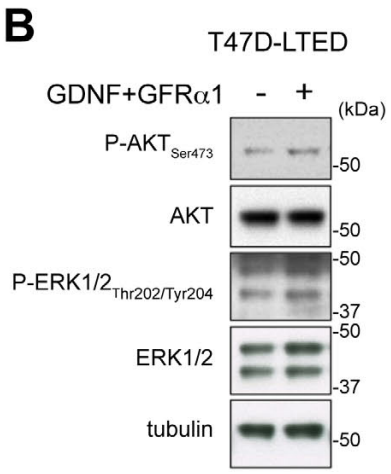
B
T47D-LTED
GDNF+GFRα1 - +
(kDa)
P-AKT Ser473
AKT
P-ERK1/2 Thr202/Tyr204
ERK1/2
tubulin

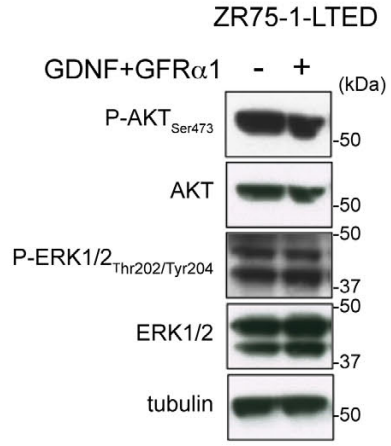
ZR75-1-LTED
GDNF+GFRα1 - +
(kDa)
P-AKT Ser473
AKT
P-ERK1/2 Thr202/Tyr204
ERK1/2
tubulin

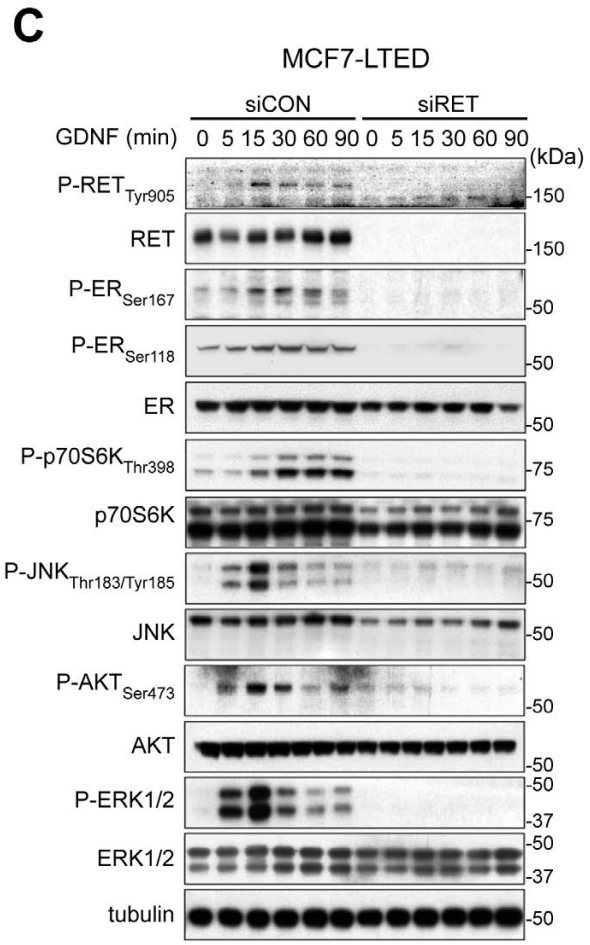
C
MCF7-LTED
siCON
siRET
GDNF (min) 0 5 15 30 60 90 0 5 15 30 60 90
(kDa)
P-RET Tyr905
RET
P-ER Ser167
P-ER Ser118
ER
P-p70S6K Thr398
p70S6K
P-JNK Thr183/Tyr185
JNK
P-AKT Ser473
AKT
P-ERK1/2
ERK1/2
tubulin

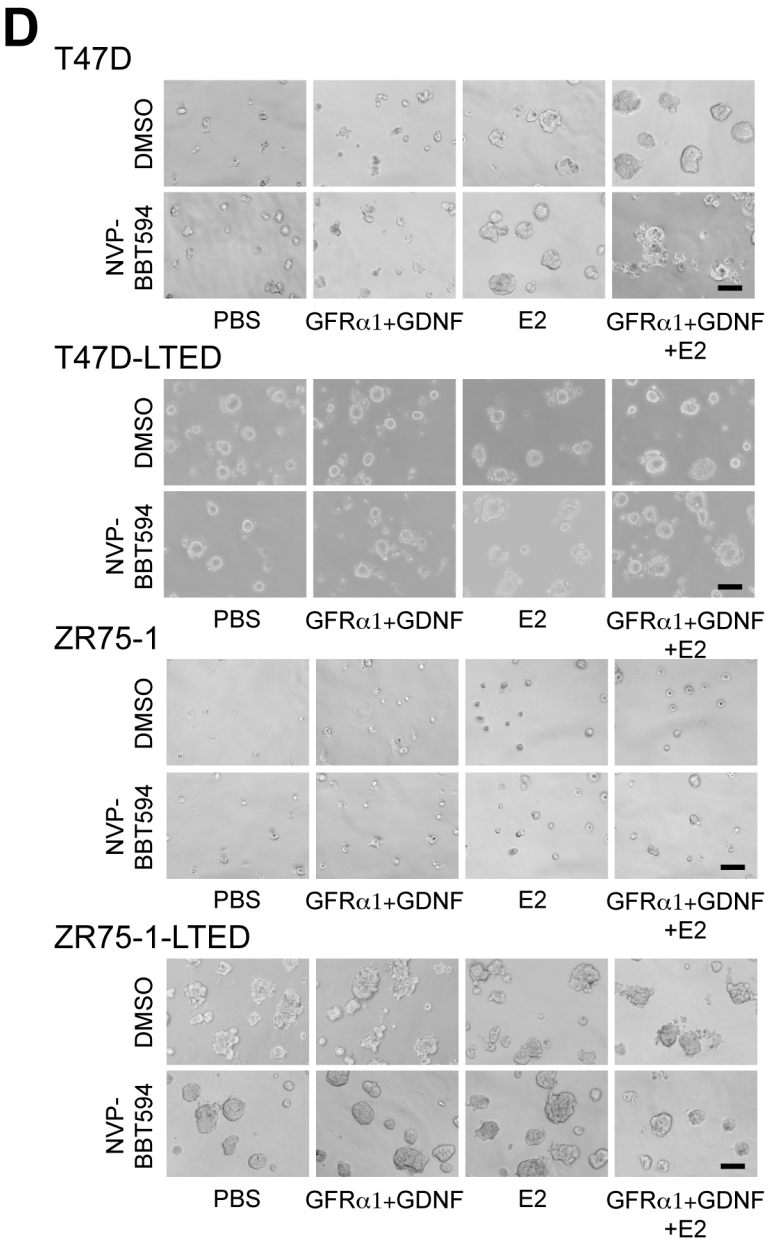

Supplementary Figure S1. Characterization of long-term E2 deprived (LTED) breast cancer cell line. A, Gene expression profiling of *RET*, *GFRA1* and *ESR1* in the ER+ breast cancer cell lines MCF7, ZR75-1 and T47D during adaptation to long-term E2 deprivation. In addition, independent data on RET expression in MCF7 cells following E2 deprivation was obtained from Aguilar *et al.* (Oncogene. 2010 Nov 11;29(45):6071-83). *RET* and *ESR1* mRNA expression following long-term E2 deprivation where confirmed by qRT-PCR and western blotting (see Fig. 1A,B). B, T47D-LTED and ZR75.1-LTED cells do not respond to GFRα1/GDNF stimulation. Cells were serum-starved overnight and stimulated with GDNF (20 ng/ml) plus GFRα1 (100 ng/ml) for 0 or 15 min. Total cell protein extracts were subject to western blotting. C, RET is essential to drive GDNF-induced signaling in MCF7-LTED cells. Cells were transfected with control (siCON) or siRET oligonucleotides. After 36 hours, cells were serum-starved overnight and stimulated with GDNF (20 ng/ml) for 0 - 90 min. Total cell protein extracts were subjected to western blotting. D, Representative phase contrast images of 3D growth assays from data shown in Figures 2C and 2D. Scale bar, 200 μm.

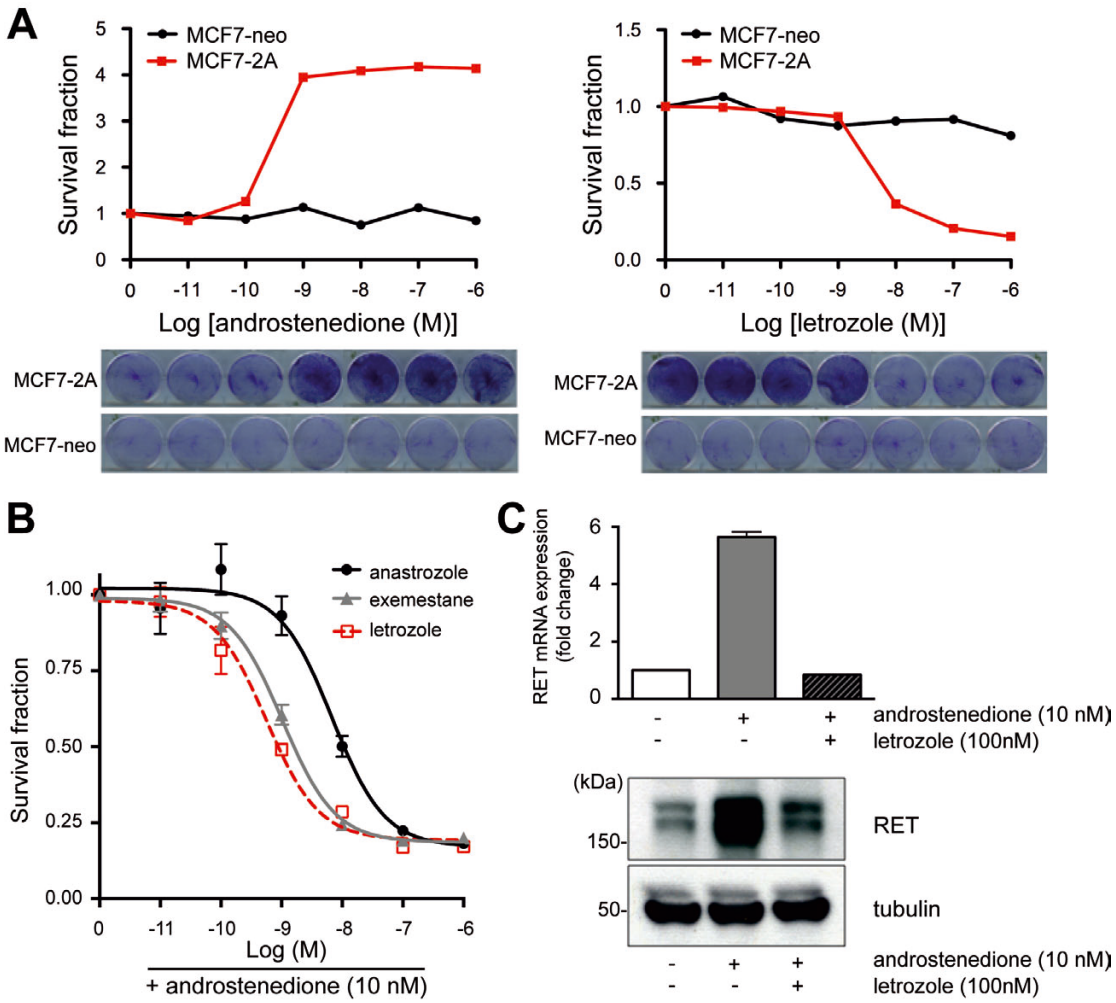
A
Survival fraction
MCF7-neo
MCF7-2A
Log [androstenedione (M)]
Log [letrozole (M)]
MCF7-2A
MCF7-neo
B
anastrozole
exemestane
letrozole
Survival fraction
Log (M)
+ androstenedione (10 nM)
C
RET mRNA expression (fold change)
androstenedione (10 nM)
letrozole (100nM)
(kDa)
150-
50-
RET
tubulin

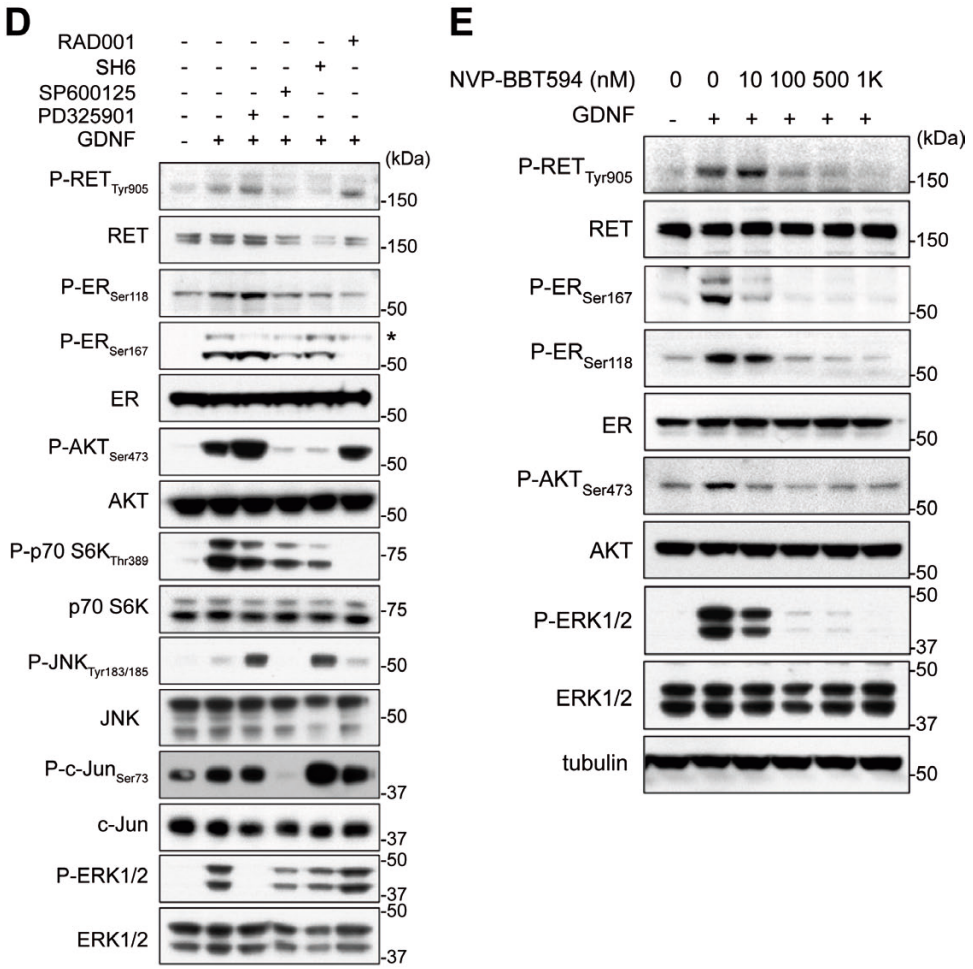

Supplementary Figure S2. Characterization of the MCF7-2A model. A, MCF7-2A and MCF7-neo cells were seeded into 12-well plates. Monolayers were treated with increasing concentrations of androstenedione (left panel) or letrozole plus 10 nM androstenedione (right panel). After 6 days, cell viability was quantified using crystal violet staining as previously described (Morandi *et al.*, PLoS One. 2011;6(11):e27450). B, MCF7-2A cells in 2D culture were E2-deprived for 3 days and then cultured in the presence of 10 nM androstenedione plus increasing concentrations of the aromatase inhibitors letrozole (open red square), exemestane (grey triangle) or anastrozole (black circle) for 6 days. Cell viability was measured using the CellTiter-Glo® assay. Data represent mean survival fraction ± SEM, n=3. C, Letrozole impairs androstenedione-induced RET expression. MCF7-2A cells in 2D culture were E2-deprived for 3 days and then stimulated for 24 hours in the presence or absence of 10 nM androstenedione, with or without 100 nM letrozole. Top panel, qRT-PCR analysis for RET (n=3). Data represents mean±SEM. Bottom panel, total cell protein extracts were subject to western blotting. D, RET signaling induces ER phosphorylation through mTOR. MCF7-2A cells were E2-deprived for 3 days, serum-starved overnight and either untreated (-) or treated (+) with the following kinase inhibitors: MEKi (PD325901 500 nM), JNKi (SP600125 10 μM), PI3Ki (SH6 10 μM), mTORi (RAD001 2 nM) or vehicle alone for 2 hours followed by GDNF stimulation (20 ng/ml, 15 min). Total cell protein extracts were subject to western blotting. E, NVP-BBT594 blocks GDNF-induced RET downstream signaling. MCF7-2A cells were E2-deprived for 3 days, serum-starved overnight and treated with 0 - 1,000 nM NVP-BBT594 for 90 min followed by GDNF stimulation (20 ng/ml, 30 min). Total cell protein extracts were subject to western blotting.

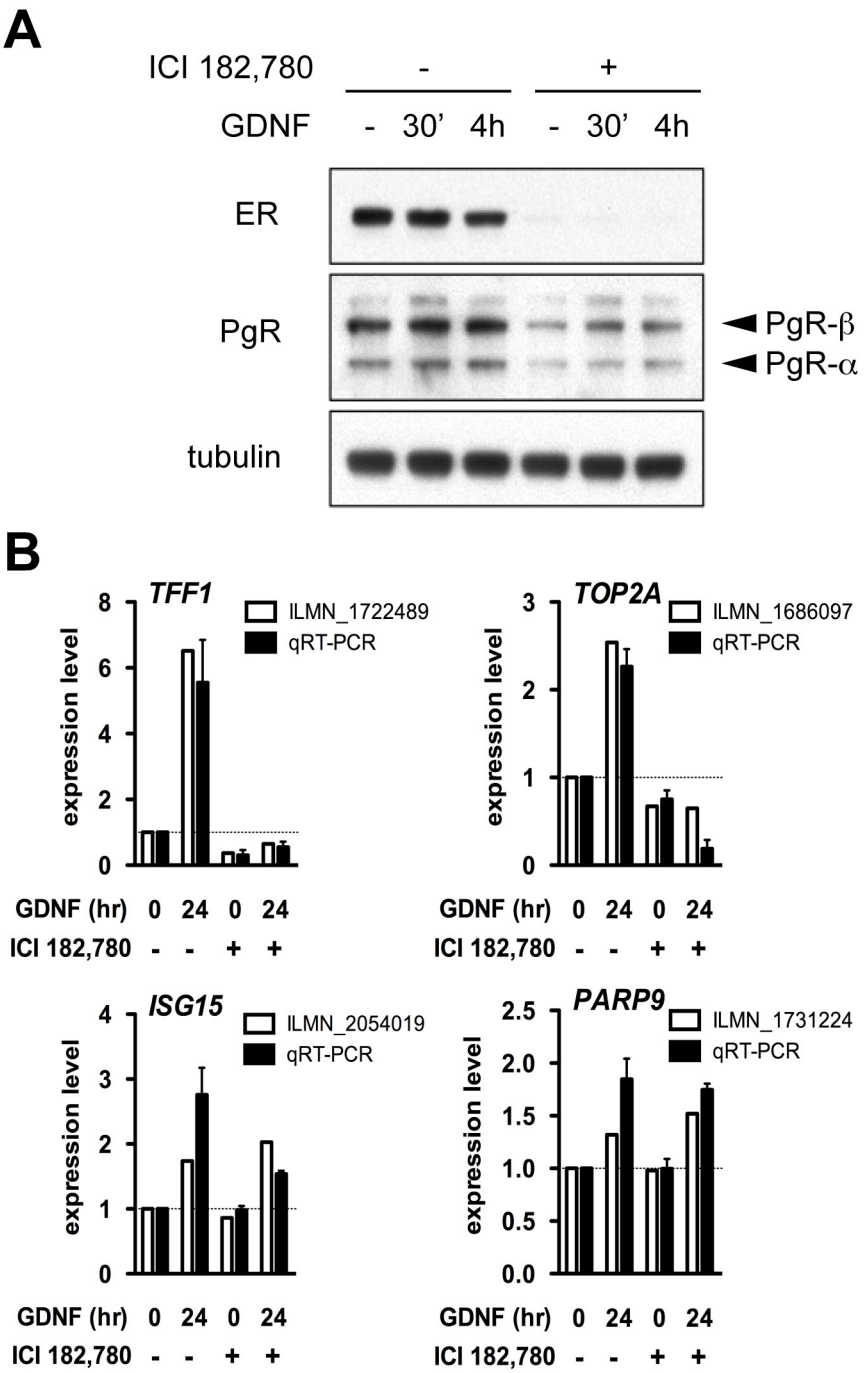

Supplementary Figure S3. Treatment of MCF7 cells with ICI 182,780 blocks ER-dependent GDNF signaling. 3 day E2-deprived MCF7 cells were serum-starved overnight in the presence or absence of 100 nM ICI 182,780 and then stimulated with GDNF (20 ng/ml) for 0 - 24 hours. A, Total cell lysates were subject to western blotting. PgR antibody (NCL-PgR 312; Novocastra) was used at a dilution of 1:500. B, qRT-PCR analysis (n = 3) was performed for *TFF1* (Hs00907239_m1), *TOP2A* (Hs00172214), *ISG15* (Hs01921425_s1) and *PARP9* (Hs00967084) (n=3). RQ expression values obtained from qRT-PCR (black bars) were compared to values retrieved from the gene expression array (white bars).

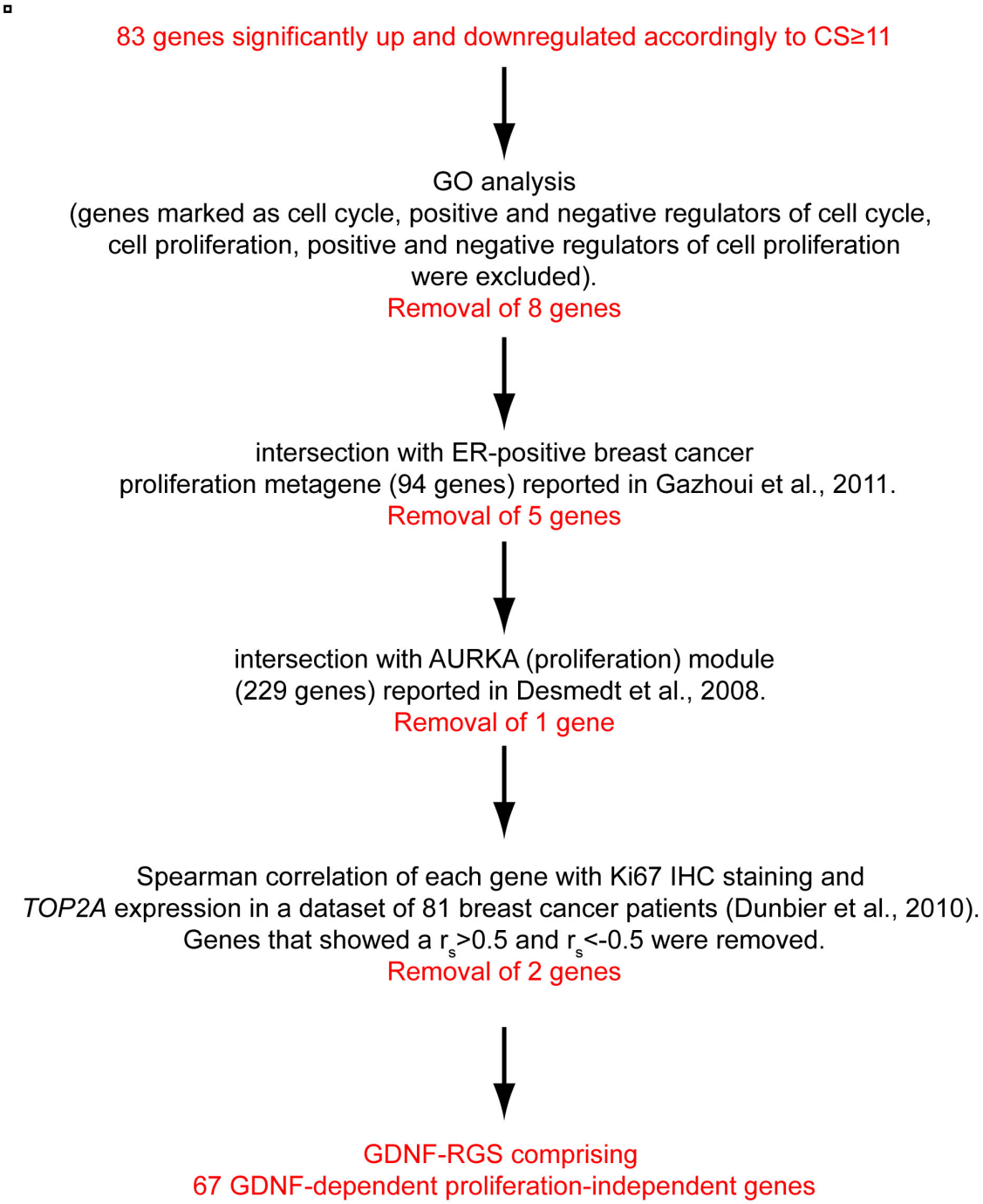

Supplementary Figure S4. Generation of the GDNF-RGS. Flowchart detailing the exclusion criteria applied to the 83 differentially regulated GDNF-dependent genes with a confidence score (CS) ≥11 to generate the proliferation-independent GDNF-response gene set (GDNF-RGS) containing 67 genes. The initial 83 gene list and the final 67 gene GDNF-RGS are listed in Supplemental Table 1B.

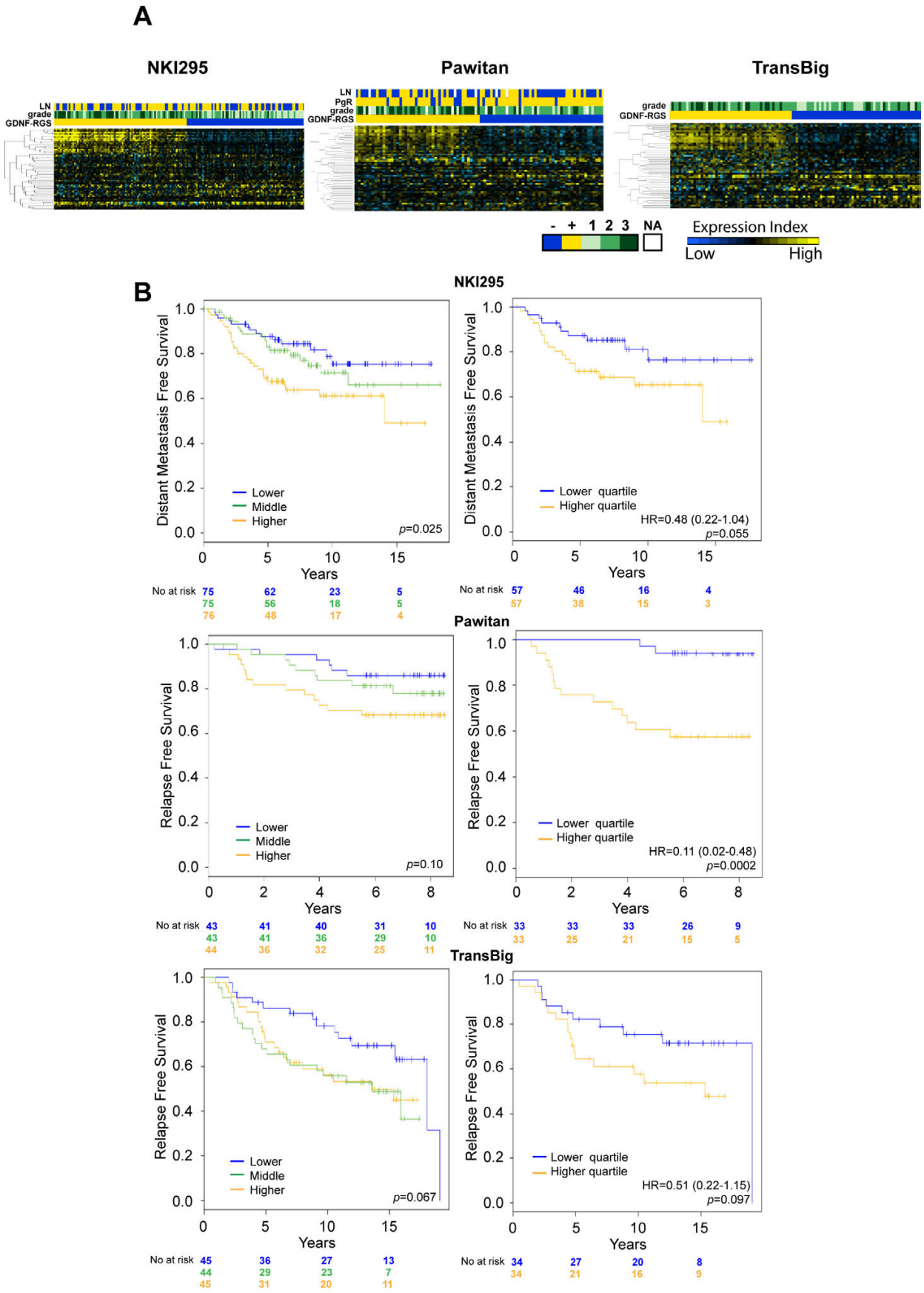
A
NKI295
Pawitan
TransBig
LN
grade
GDNF-RGS
PgR
- + 1 2 3 NA
Expression Index
Low
High
B
NKI295
Distant Metastasis Free Survival
Lower
Middle
Higher
p=0.025
Lower quartile
Higher quartile
HR=0.48 (0.22-1.04)
p=0.055
Years
No at risk 75 62 23 5
75 56 18 5
76 48 17 4
No at risk 57 46 16 4
57 38 15 3
Pawitan
Relapse Free Survival
p=0.10
HR=0.11 (0.02-0.48)
p=0.0002
No at risk 43 41 40 31 10
43 41 36 29 10
44 36 32 25 11
No at risk 33 33 33 26 9
33 25 21 15 5
TransBig
p=0.067
HR=0.51 (0.22-1.15)
p=0.097
No at risk 45 36 27 13
44 29 23 7
45 31 20 11
No at risk 34 27 20 8
34 21 16 9

Supplementary Figure S5. GDNF-RGS positivity correlates with poor outcome in human breast cancer. A, Heat map of GDNF-RGS genes in the NKI295, Pawitan and TransBig datasets analyzed in Figure 5. Patients were divided into GDNF-RGS+ and GDNF-RGS- using the centroid correlation method as reported in the main text. LN: Lymph node status. NA: Not available. B, GDNF-RGS correlates with poor prognosis in human breast cancers. Kaplan-Meier analyses of distant metastases free survival or relapse free survival in the NKI295, Pawitan and TransBig breast cancer datasets. In the left panels, cases were divided into equally sized tertiles based on their GDNF-RGS score. In the right panels, cases were divided into equally sized quartiles. The higher (top 25%) and lower (bottom 25%) quartiles are shown. Likelihood ratio test p-value and hazard ratio (HR) with 95% confidence interval are shown in each panel.

A

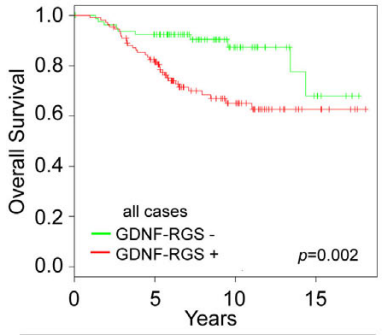

Variable	HR	95% CI	p
GDNF-RGS	2.35	1.13-4.85	0.021
Tumor size (>20 vs ≤ 20 mm)	2.68	1.41-5.09	0.003
Lymph node status	0.84	0.45-1.57	0.598
Age (>50 vs ≤ 50 yrs)	0.76	0.31-1.86	0.551
ER status	0.60	0.29-1.23	0.160

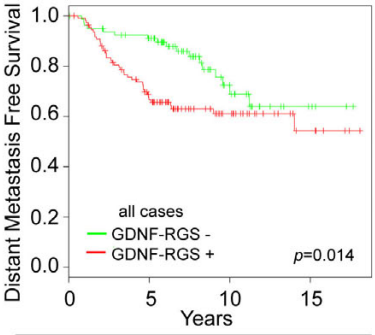

Variable	HR	95% CI	p
GDNF-RGS	1.81	1.00-3.25	0.047
Tumor size (>20 vs ≤ 20 mm)	2.54	1.46-4.41	0.001
Lymph node status	0.70	0.41-1.21	0.202
Age (>50 vs ≤ 50 yrs)	0.67	0.31-1.52	0.343
ER status	0.82	0.41-1.65	0.594

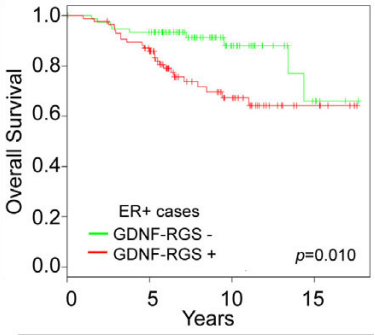

Variable	HR	95% CI	p
GDNF-RGS	2.56	1.18-5.55	0.017
Tumor size (>20 vs ≤ 20 mm)	2.05	1.01-4.16	0.045
Lymph node status	0.77	0.38-1.55	0.466
Age (>50 vs ≤ 50 yrs)	0.69	0.26-1.83	0.459

B

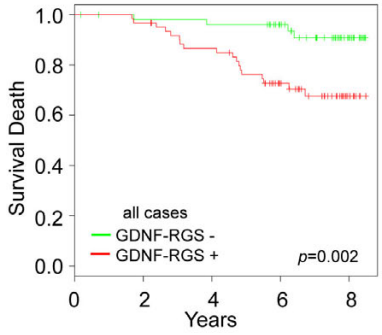

Variable	HR	95% CI	p
GDNF-RGS	4.61	1.39-15.24	0.012
Grade (3 vs 2/1)	1.15	0.43-3.08	0.788
Lymph node status	0.69	0.25-1.92	0.480
Age (>50 vs ≤ 50 yrs)	0.456	0.18-1.16	0.099
Tumor size (>20 vs ≤ 20 mm)	3.94	1.44-10.75	0.008
PgR status	0.78	0.25-2.49	0.678
ER status	1.42	0.32-6.25	0.644

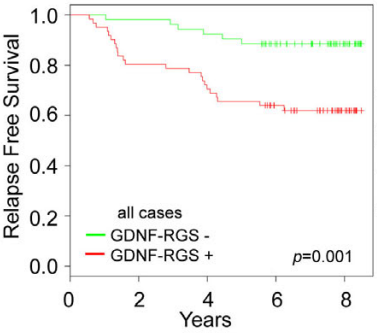

Variable	HR	95% CI	p
GDNF-RGS	3.31	1.24-8.86	0.017
Grade (3 vs 2/1)	1.22	0.51-2.93	0.659
Lymph node status	0.61	0.26-1.45	0.267
Age (>50 vs ≤ 50 yrs)	0.33	0.14-0.78	0.011
Tumor size (>20 vs ≤ 20 mm)	2.61	1.09-6.25	0.031
PgR status	0.78	0.27-2.20	0.635
ER status	0.85	0.26-2.81	0.7885

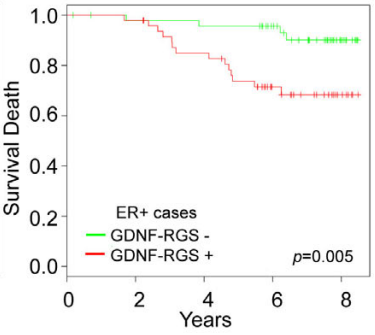

Variable	HR	95% CI	p
GDNF-RGS	4.28	1.27-14.48	0.019
Grade (3 vs 2/1)	1.38	0.49-3.93	0.545
Lymph node status	0.60	0.18-1.95	0.393
Age (>50 vs ≤ 50 yrs)	0.43	0.16-1.17	0.099
Tumor size (>20 vs ≤ 20 mm)	3.91	1.24-12.40	0.020
PgR status	0.96	0.26-3.49	0.950

C

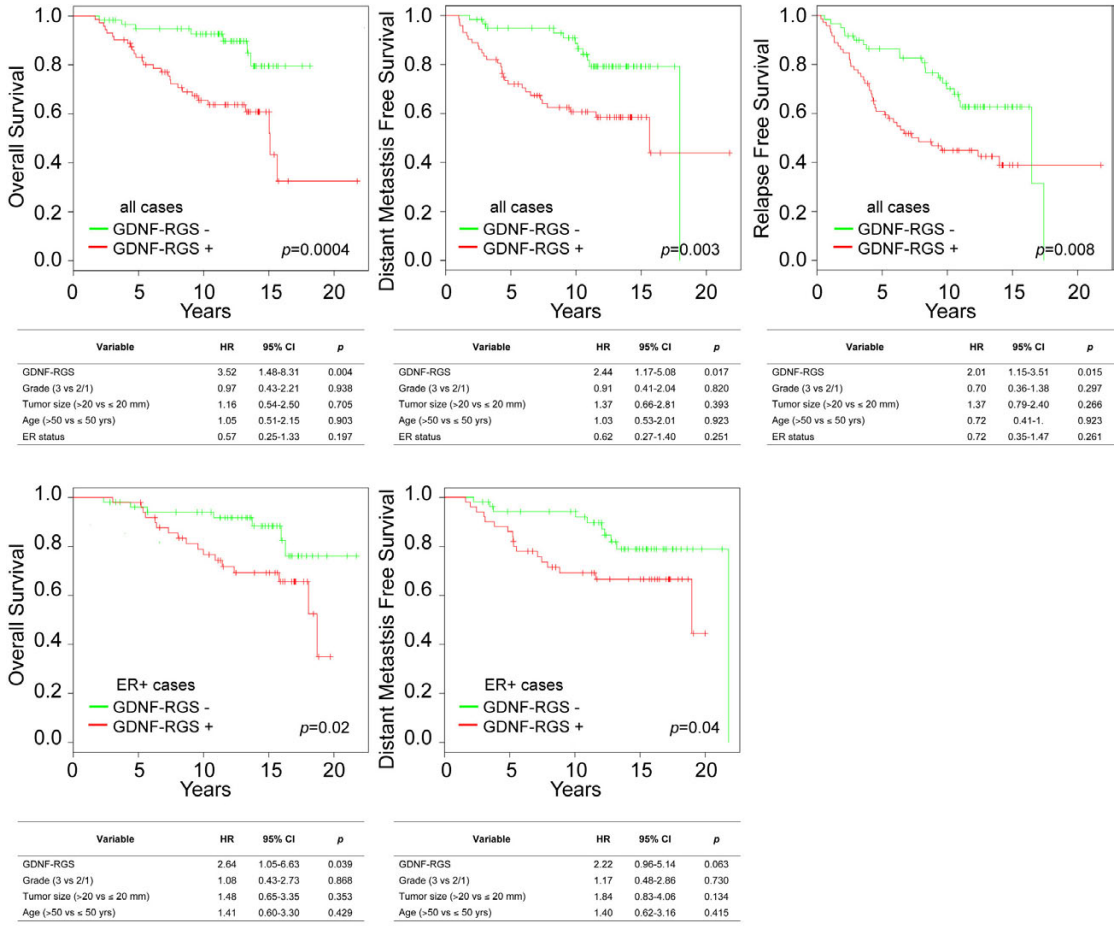

Variable	HR	95% CI	p
GDNF-RGS	3.52	1.48-8.31	0.004
Grade (3 vs 2/1)	0.97	0.43-2.21	0.938
Tumor size (>20 vs ≤ 20 mm)	1.16	0.54-2.50	0.705
Age (>50 vs ≤ 50 yrs)	1.05	0.51-2.15	0.903
ER status	0.57	0.25-1.33	0.197

Variable	HR	95% CI	p
GDNF-RGS	2.44	1.17-5.08	0.017
Grade (3 vs 2/1)	0.91	0.41-2.04	0.820
Tumor size (>20 vs ≤ 20 mm)	1.37	0.66-2.81	0.393
Age (>50 vs ≤ 50 yrs)	1.03	0.53-2.01	0.923
ER status	0.62	0.27-1.40	0.251

Variable	HR	95% CI	p
GDNF-RGS	2.01	1.15-3.51	0.015
Grade (3 vs 2/1)	0.70	0.36-1.38	0.297
Tumor size (>20 vs ≤ 20 mm)	1.37	0.79-2.40	0.266
Age (>50 vs ≤ 50 yrs)	0.72	0.41-1.	0.923
ER status	0.72	0.35-1.47	0.261

Variable	HR	95% CI	p
GDNF-RGS	2.64	1.05-6.63	0.039
Grade (3 vs 2/1)	1.08	0.43-2.73	0.868
Tumor size (>20 vs ≤ 20 mm)	1.48	0.65-3.35	0.353
Age (>50 vs ≤ 50 yrs)	1.41	0.60-3.30	0.429

Variable	HR	95% CI	p
GDNF-RGS	2.22	0.96-5.14	0.063
Grade (3 vs 2/1)	1.17	0.48-2.86	0.730
Tumor size (>20 vs ≤ 20 mm)	1.84	0.83-4.06	0.134
Age (>50 vs ≤ 50 yrs)	1.40	0.62-3.16	0.415

Supplementary Figure S6. Kaplan-Meier analyses for breast cancer cases stratified by GDNF-RGS. Patients were divided into GDNF-RGS+ and GDNF-RGS- using the centroid correlation method as reported in the main text. Graphs show Kaplan-Meier analyses for all cases and ER+ cases in the (A) NKI295, (B) Pawitan and (C) TransBig datasets. Tables show relative multivariate Cox proportional-hazard regression analyses according to the GDNF-RGS adjusted for traditional prognostic clinico-pathological factors. Likelihood ratio test p-value is shown in each panel.

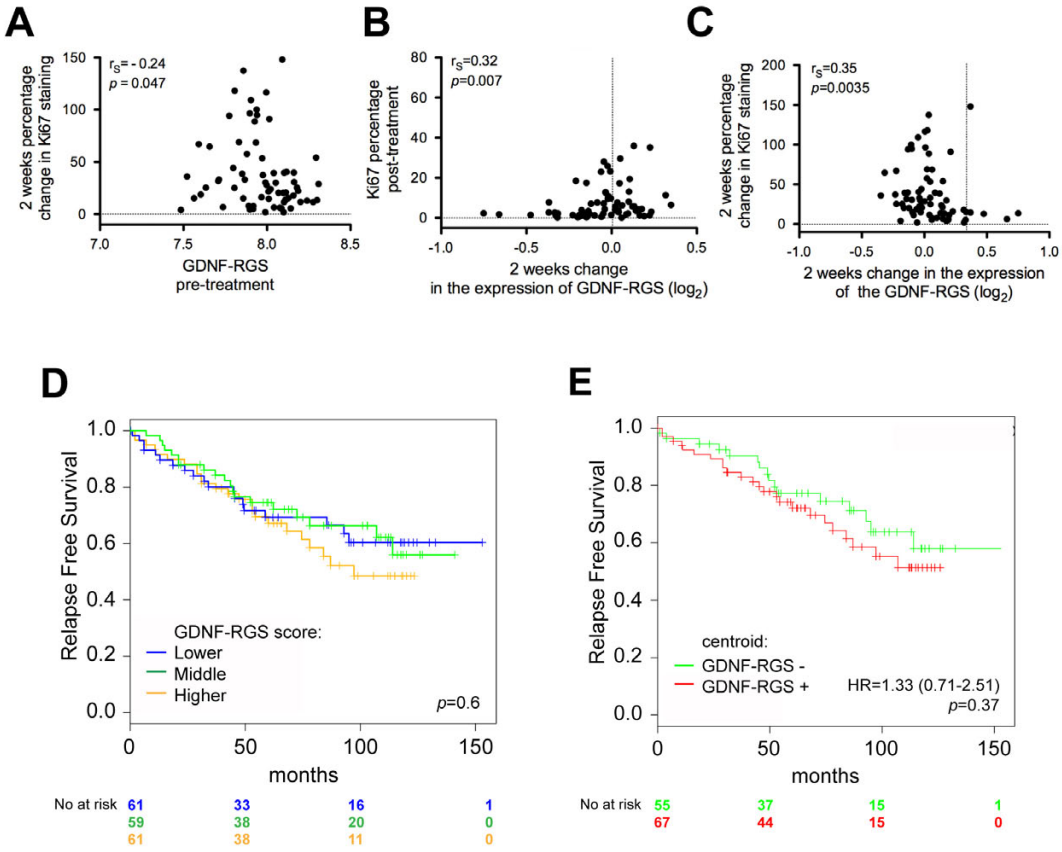

Supplementary Figure S7. (A-C) Correlation of GDNF-RGS with Ki67 staining following anastrozole treatment. Data is from 81 ER+ breast carcinomas from which biopsies were taken at pre- and post- 2 weeks neoadjuvant anastrozole treatment (Dunbier *et al*., 2010). Of the 81 patients, paired pre- and post-treatment gene expression profiles and Ki67 immunohistochemical staining were available for 69 patients. 61 out of 67 of the GDNF-RGS genes were available in the FAIMoS data set and log2 intensity values were used. GDNF-RGS pre-treatment score and changes of GDNF-RGS pre- and post-treatment were correlated to Ki67 levels and Ki67 changes after treatment using Spearman correlation as previously reported (Ghazoui et al., 2011). A, GDNF-RGS pre-treatment score showed a relatively weak but statistically significant correlation with the proportional two-week change in Ki67. B and C, comparison of the 2-week change in GDNF-RGS with (B) Ki67 staining in the post-treatment biopsies, and (C) the change in Ki67 staining between pre- and post-treatment biopsies. No correlation was found between GDNF-RGS and Ki67 expression in pre-treatment primary samples (rs=-0.09, p=0.46). (D, E) GDNF-RGS is not predictive for tamoxifen response in human breast cancers. 10 publically available Affymetrix HG-U133A gene chip gene expression studies (GSE2034, GSE11121, GSE20194, GSE1456, GSE2603, GSE6532, GSE20437, E-TABM-185, GSE7390, GSE5847) were retrieved using ROCK database (rock.icr.ac.uk) (and called Ur-Rehman). This approach allowed us to generate a homogeneous dataset of breast cancer patients treated with tamoxifen by (i) retrieving raw data from public databases, (ii) quality control check and (iii) Robust Multi-array Averaging (RMA) normalization and log2 transformation. Kaplan-Meier analyses for 181 ER positive tamoxifen treated breast cancer cases stratified by GDNF-RGS are shown. D, Patients were assigned into equally sized tertiles on their GDNF-RGS score. E,

Patients were divided into GDNF-RGS+ and GDNF-RGS- using the centroid correlation method as reported in the main text. 59 patients were not assigned to either GDNF-RGS+ or GDNF-RGS- if the correlation was ≤0.1 as described in the main text. No significant differences were found between the 2 groups. Likelihood ratio test p-value (A, B) and hazard ratio (HR) with 95% confidence interval (B) are shown.

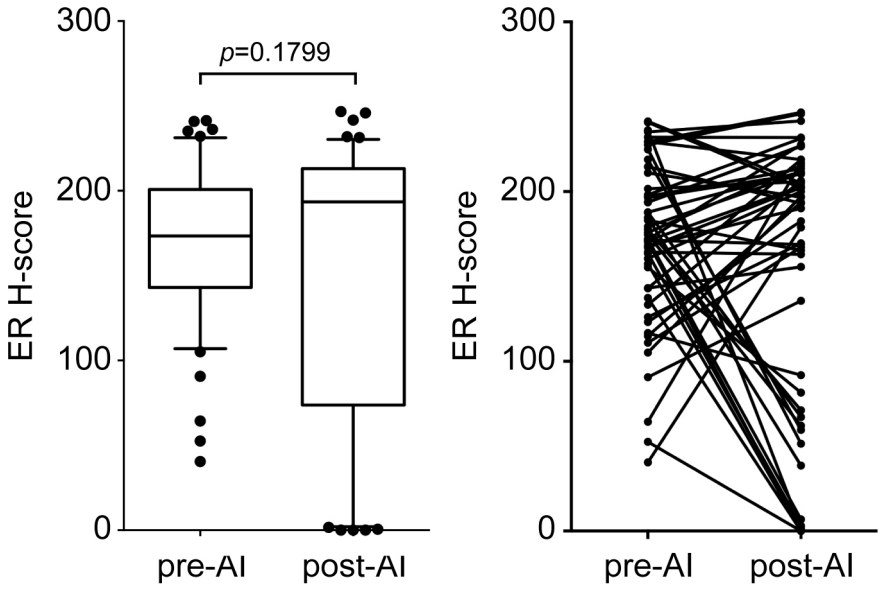

Supplementary Figure S8. ER H-score values in 52 paired primary tumor samples pre-aromatase inhibitor treatment (pre-AI) and recurrent/metastatic tumors following adjuvant AI treatment (post-AI). See Weigel *et al.*, 2012 for the clinical and pathological patient information. There was no significant change in ER H-score between pre-AI and post-AI samples. Left panel, box and whisker plots represent median, 10 and 90 percentile values. Dots represent the outliers. Right panel, changes in ER H-score in 52 paired ER+ breast cancer samples pre- and post-AI treatment.